Effects of Biphenyl Polymerization on Lithium Deposition in Commercial Graphite/NMC Lithium-Ion Pouch-Cells during Calendar Aging at High Temperature

Bramy Pilipili Matadi,[a,b] Sylvie Geniès,[c,d] Arnaud Delaille,[a,b,z] Thomas Waldmann,[e] Michael Kasper,[e] Margret Wohlfahrt-Mehrens,[e] Frederic Aguesse,[f] Emilie Bekaert,[f] Isabel Jiménez-Gordon,[c,d] Lise Daniel,[c,d] Xavier Fleury,[c,d] Michel Bardet,[g] Jean-Frédéric Martin,[c,d] and Yann Bultel[h,i]

[a] *University Grenoble Alpes, INES, F-73375 Le Bourget du Lac, France*
[b] *CEA, LITEN, DTS, F-38054 Grenoble, France*
[c] *University Grenoble Alpes, F-38000 Grenoble, France*
[d] *CEA, LITEN, DEHT, F-38054 Grenoble, France*
[e] *ZSW - Zentrum für Sonnenenergie- und Wasserstoff-Forschung Baden-Württemberg, D-89081 Ulm, Germany*
[f] *CIC EnergiGUNE, Parque Tecnológico de Álava, 01510 Miñano, Spain*
[g] *CEA, DRF/INAC, MEM, RM, F-38054 Grenoble, France*
[h] *University Grenoble Alpes, LEPMI, F-38000 Grenoble, France*
[i] *CNRS, LEPMI, F-38000 Grenoble, France*

Metallic lithium deposition is a typical aging mechanism observed in lithium-ion cells at low temperature and/or at high charge rate. Lithium dendrite growth not only leads to strong capacity fading, it also causes safety concerns such as short-circuits in the cell. In applications such as electric vehicles, the use of lithium-ion batteries combines discharging, long rest time and charging phases. It is foremost a matter of lifetime and safety from the perspective of the consumer or the investor.

This study presents the post-mortem analyses of commercial 16 Ah Graphite/NMC (Nickel Manganese Cobalt layered oxide) Li-ion pouch cells. The cells were degraded by calendar aging at high temperature with or without periodic capacity tests. Unexpected local depositions of metallic lithium were confirmed on graphite electrodes by Nuclear Magnetic Resonance (NMR). Biphenyl, a monomer additive present in the liquid electrolyte, generates gas during its polymerization reaction occurring at high temperature and at high state of charge. As a result, dry-out areas are present between the electrodes leading to high impedance regions and no charge transfer between the electrodes. It is at the border of these areas that lithium metal is deposited.

© The Author(s) 2017. Published by ECS. This is an open access article distributed under the terms of the Creative Commons Attribution 4.0 License (CC BY, http://creativecommons.org/licenses/by/4.0/), which permits unrestricted reuse of the work in any medium, provided the original work is properly cited. [DOI: 10.1149/2.0631706jes] All rights reserved.

Manuscript submitted January 10, 2017; revised manuscript received February 17, 2017. Published March 25, 2017. This was Paper 927 presented at the Honolulu, Hawaii, Meeting of the Society, October 2–7, 2016.

Lithium-ion batteries have the particularity of addressing applications as diverse as mobile electronic devices, electric vehicles or stationary applications of renewable energy. The use of rechargeable electrochemical cells is first and foremost a question of autonomy, lifetime and safety.[1–3] So it is necessary to further increase the current performance of lithium-ion batteries.

Deposition of metallic lithium or "lithium plating" is one of the aging mechanisms that is limiting the lifetime of lithium-ion batteries.[4–20] In the literature, it is reported that the mechanism of lithium deposition generally occurs during the charge at low temperatures and/or at high current-rates. The intercalation of lithium ions into the structure of the negative electrode is in competition with the deposition of metallic lithium on top of the Solid Electrolyte Interphase (SEI). The morphology of the negative electrode, the porosity, the conductivity of the electrolyte and the state of lithiation are parameters to be considered.[8] This aging mechanism depends on intrinsic criteria of the components of the cell (active material, electrodes and electrolyte composition[21–30]) and extrinsic to the system (temperature and charging current).

Contact between the deposited lithium and the electrolyte (above the surface of the SEI) leads to the oxidation of lithium to form species such as $ROCO_2Li$, Li_2CO_3 or LiF.[15] The deposited lithium becomes isolated and electrochemically inactive and cannot participate in the electrochemical process at the electrodes. The deposit can grow in height from graphite particles and form dendrites which can pass through the separator and cause short circuit. This phenomena in combination to flammable solvents can produce an exothermic reaction, leading to a violent destruction of the cell during thermal runaway.[31] This represents a considerable safety risk for the battery. Sometimes, metallic lithium, although still active, can be electronically disconnected from the electrode and is thus unusable ("dead lithium").[4,5,10,17] This lithium loss contributes to progressive and irreversible capacity fading.

Graphite is one of the most common negative electrodes and presents plateaus of intercalation / deintercalation between 0.05 and 0.1 V vs. Li/Li^+,[32–35] while below 0 V vs Li/Li^+ lithium metal forms. The detection of metallic lithium deposition is possible by measuring the potential of the negative electrode using a reference electrode. Nevertheless, only post-mortem analyses can really confirm the presence of metallic lithium on the electrodes. Jalkanen et al.[20] suggested the presence of lithium deposition after cycling at high temperature. Ghanbari et al.[36] showed that metallic lithium can be observed using glow discharge optical emission spectroscopy (GD-OES) depth profiling. As far as we know, there is no published results reporting lithium plating at high temperature operating conditions during calendar aging.

This paper presents the relation between metallic lithium depositions and the stability of the electrolyte components in a commercial Graphite/NMC Li-ion cell, observed rather unexpectedly at high temperature and high state of charge conditions.

Post mortem analysis revealed the presence of localized Li metal depositions on the surface of the graphite electrodes. The effects of the liquid electrolyte components, and more particularly the biphenyl additive, identified by Gas Chromatography – Mass Spectrometry (GC-MS), are investigated. Biphenyl is a monomer additive in the electrolyte used as a fire-retardant in lithium-ion batteries.[9,25] Solid state NMR is used to characterize areas presenting Li deposition. Coin cells based on pristine electrodes are assembled to study the influence of this aromatic compound in the electrolyte and to identify the relation between the periodic check-ups and the metallic lithium deposition.

Experimental

In this study, we use commercial Li-ion pouch cells with a nominal capacity of 16 Ah, an energy density of 146 Wh/kg, a mass of 406 g,

[z] E-mail: arnaud.delaille@cea.fr

and a voltage range of 2.7–4.2 V. These commercial 16 Ah Li-ion batteries contain 23 bifacial and 2 single-facial positive electrodes and 24 bifacial negative electrodes. Graphite and Nickel Manganese Cobalt oxide ($Li_x(Ni_{0.41}Mn_{0.37}Co_{0.22})O_2$.) are the negative and positive electrodes, respectively. The separator is composed of polyethylene with a porous PVDF-HFP coating layer. VDF is the amorphous part of the polymer and can trap the electrolyte (increase of the ionic conductivity of the separator) while HFP constitutes the crystalline part, which provides a mechanical support (improvement of the mechanical properties of the separator).

Cells are aged in calendar mode using 3 different states of charge (SOC), namely SOC=50%, 90% and 100% and 4 different temperatures, namely T=5°C, 25°C, 45°C and 60°C. In order to measure the capacity of the cell, periodic check-ups are performed at 25°C every 8 weeks for cells stored at 5°C and 25°C, every 6 weeks for cells stored at 45°C and every 4 weeks for cells stored at 60°C. It is well known that the calendar aging of Li-ion batteries is accelerated by high state of charge and high temperature conditions during storage time.[37,38] That is why we decided to manage the periodicity of the experimental control tests, which consists in reducing the time between two check-ups for more severe aging conditions in order to limit the decrease in capacity between the two tests (and conversely for less severe aging conditions). Electrochemical periodic check-up tests are performed with a Digatron System according to the following protocol: residual discharge performed at a rate of 1 C followed by charge/discharge cycles performed at a rate of C/25 and then at rate of 1 C.

An additional cell was stored (T=60°C, SOC=100%) without any periodic electric check-up tests during 4 months. The duration corresponds to time of storage of other cells aged at 60°C. In this case, a test of capacity is performed at low charge rate at 25°C before and after the 4 months of storage according to the following protocol: residual discharge performed at a rate of C/25 until 2.7 V. After a rest of 30 minutes, a charge is performed at rate of C/25 until 4.2 V followed by a last discharge at C/25 until 2.7 V. Here, the aim is to measure the influence of intermediate check-ups on the aging. The low charge of C/25 has been used instead of both rates of 1 C and C/25, in order to observe the impact of the charge rate of 1 C on the aging. A previous study with the same cell type showed that charging at C/25 does not lead to negative anode potentials vs. Li/Li^+ and therefore no Li deposition is expected.[18]

Standard electrochemical measurements are performed in order to characterize cells before dismantling. Cells are discharged at a rate of C/10 until 2.7 V is reached. The same discharge procedure is repeated after a rest of 5 minutes. This discharge procedure is performed 3 hours before the cell opening. Cell sizes are measured in order to check for size variation and hint for gas generation. The pouch cells are opened using a ceramic knife in an Argon-filled glove box for safety reasons. Careful cuts are realized avoiding shortcuts between electrodes to obtain reliable results. The electrode pairs in the middle of the pouch cells are considered for analysis.

Lithium-7 nuclear magnetic resonance (NMR) technique is used to detect metallic lithium on graphite electrodes.[39,40] Solid-state MAS NMR measurements were performed on a Brucker AVANCE DSX 200 MHz spectrometer (4.7 T, ^{7}Li Larmor frequency $\nu_0 = 77.78$ MHz) equipped with a 1.3 mm Bruker CPMAS probe head. The ^{7}Li MAS NMR spectra were recorded at different MAS spinning frequencies in the range 36–60 kHz with either direct ^{7}Li excitation or a rotor-synchronized Hahn echo pulse sequence (90° - τ - 180° - τ – acq, where $\tau = 1/\nu_{rot}$). Different repetition delays for transient accumulation were tested in the range of 1 to 30 s in order to obtain quantitative data. A ^{7}Li 90°-pulse width of 3 μs was used, corresponding to the nucleus magnetization turn angle of about 75–80°. High power proton decoupling was also used but did not improve the quality of the spectra since proton and lithium are not directly linked neither through bond nor through space interactions. All spectra were acquired with room temperature bearing air, corresponding to a sample temperature in the range 50–70°C. Aqueous LiCl solution was used as a chemical shift reference set to 0 ppm. Inside a glove box different samples were collected by scraping electrodes (previously washed twice with Dimethyl carbonates (DMC)) on the base of visual observation. A sample of lithium metal was recorded in order to measure its chemical shift (265 ppm). For illustration of ionic lithium a sample of Li_3PO_4 was also recorded.

GC-MS was performed on samples harvested from the electrolyte. During the cell opening, a piece of separator was immersed in CH_3CN as a carrier solvent for at least 2 hours. The solution is then transported to the GC-MS split/splitless injector without air exposure. We note that the probability of some components of the electrolyte being quickly volatilized during the opening of the cell under Argon atmosphere is not negligible. The list of components identified from the fresh electrolyte is consequently not exhaustive.

Coin cells are used to investigate the effect of the biphenyl additive in the electrolyte. Two types of CR2032 coin cells with pristine NMC-based electrode (cathode), pristine graphite-based electrode (anode) and Celgard 2400 separator are assembled. The first coin cell is based on 1:1:1: wt EC:DMC:EMC + 1 M $LiPF_6$ electrolyte (LPX). The second coin cell contains the same electrolyte (LPX) with additional 2wt% of biphenyl. Before aging, a formation cycle at 25°C under galvanostatic charge-discharge cycle (voltage range: 2.7–4.2 V) then C/2 in CC-CV charge was performed. The CV mode starts when the cell voltage reaches the maximum of 4.2 V and stops when the current drops to C/50. Coin cells were stored at 45°C at 100% of SOC for 25 days. The calendar phase includes a periodic electric check-up test performed at 25°C every 4 days.

Cyclic voltammetry measurements have been performed in order to measure the voltage of the biphenyl polymerization at elevated temperatures. Three additional coin-cells with pristine NMC-based electrode (cathode), metal lithium based electrode (anode), Celgard 2400 separator and 1:1:1 wt EC:DMC:EMC + 1M $LiPF_6$ electrolyte with 2wt% of biphenyl are assembled. Cyclic measurements are performed with a Biologic system between 3 and 5.2 V with a rate of 1 mV/s respectively at 25°C, 35°C and 45°C. At the end, coin cells were disassembled in an Argon-filled glove box for visual inspection in a discharged state.

Results

Aging performance.—The evolution of the SOH of the 16 Ah calendar aged commercial batteries is presented in Figure 1. These measurements were performed within the MAT4BAT project. It can be observed that the degradation of Graphite/NMC Li-ion batteries in calendar aging mode is favored by high state of charge and high temperature storage conditions. These results are consistent with

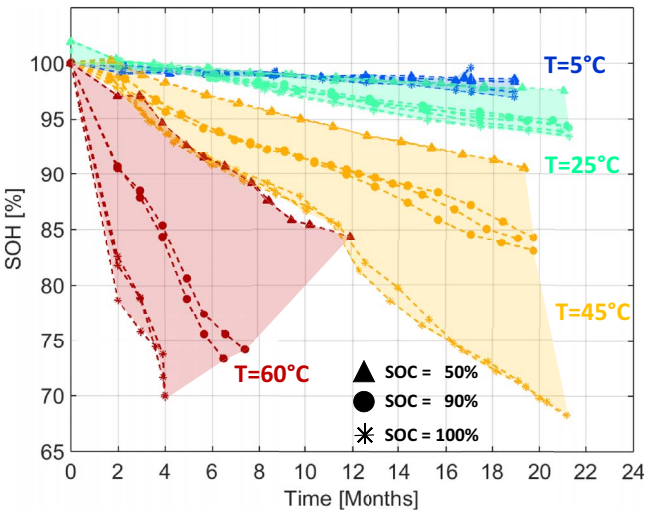

Figure 1. Evolution of the state of health of 16Ah commercial Li-ion cells in calendar aging. The reference capacity is the discharged capacity measured during periodic check-up tests at a rate of 1 C.

Calendar ageing SOC=100%		Components			Comments
		Graphite	Separator	NMC	
With periodic check-up tests	T=5°C SOH (1C)=100% Duration = 9 months				No Lithium deposition
	T=25°C SOH (1C)=100% Duration = 9 months				No Lithium deposition
	T=45°C SOH (1C)=93% Duration = 10 months				Lithium deposition
	T=60°C SOH (1C)=72% SOH (C/25)=75% Duration = 4 months	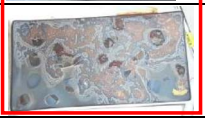			Lithium deposition
Without periodic check-up tests	T=60°C SOH (C/25)=82% Duration = 4 months				No Lithium deposition

Figure 2. Visual inspection of negative and positive electrodes and separators of commercial 16Ah Graphite/NMC pouch cells aged in calendar mode (SOC = 100%) with or without periodic electric tests. Metallic lithium depositions are found on the surface of graphite electrodes retrieved from cells stored at T=45°C and T=60°C with check-up test periods.

previously reported results.[41–44] For high temperatures, the strong difference observed between SOC=90% and SOC=100% in calendar ageing of Graphite/NMC Li-ion cells has already been observed in the literature. The influence of the SOC on the ageing is not linear with the SOC. The main hypothesis is the influence of the corresponding voltages.[37,38] The cells aged at SOC=100% and at 5°C, 25°C, 45°C and 60°C have been selected for further post-mortem analyses.

Post-Mortem Analysis of 16 Ah Pouch Cells

Visual inspection.—Visual inspection of aged components has raised several interesting features as shown in Figure 2. The electrodes and the separator are still wetted by the electrolyte at the moment of dismantling, at any aging condition. Electrodes and separator aged in the calendar condition at low temperature (T = 5°C) present no visible change. This is in accordance with the low capacity loss observed at 5°C (see Figure 1).

For the cells stored at 25°C, the separator presents a light brown color on the side in contact with positive electrodes whereas there is no notable visible change detected on the electrodes.

Harvested positive electrodes of cells stored at 45°C present a black color with circular gray stains. The separator presents a brown color with white circular areas. Graphite electrodes present concentric lithiated deposits which are symmetric to the circumference of white zones found on the brown separators and gray stains found on NMC electrodes. This symmetrical correlation between separator white zones, stains on NMC electrodes on one side and circular lithiated deposits on graphite on the other side is exposed in Figure 3. Those lithiated deposits, insoluble with DMC or acetonitrile, can be removed with friction and are very reactive with water. This is due to the presence of metallic lithium as presented in the following section.

Inside of some of these concentric lithiated deposits, the graphite appears to have a high lithiated state compared to the rest of the surface. This indicates that lithium is no more exchangeable in those areas where graphite particles remained lithiated despite the discharge before dismantling. During storage those lithiated areas were certainly strongly insulated by the contact with the driest white areas of the separator.

Similar observations are confirmed on the cells aged in calendar mode at higher temperature but are more pronounced for cells stored at 60°C with periodic check-up tests. In this cell, the graphite electrode reveals an important concentration of Li metal deposition around the symmetrical areas.

Additionally to the cells aged with periodic check-ups, a cell was aged at 60°C and SOC=100% without check-ups as detailed in the Experimental section. The post mortem study reveals that the brown



Figure 3. Calendar aging at T=45°C and at SOC=100%. Dismantling at SOH = 93% after 10 months of storage including periodic check-up tests. Symmetrical correlation between white zones on the separator and gray stains found on NMC electrodes on one side, and circular lithiated deposits on graphite electrodes on the other side.

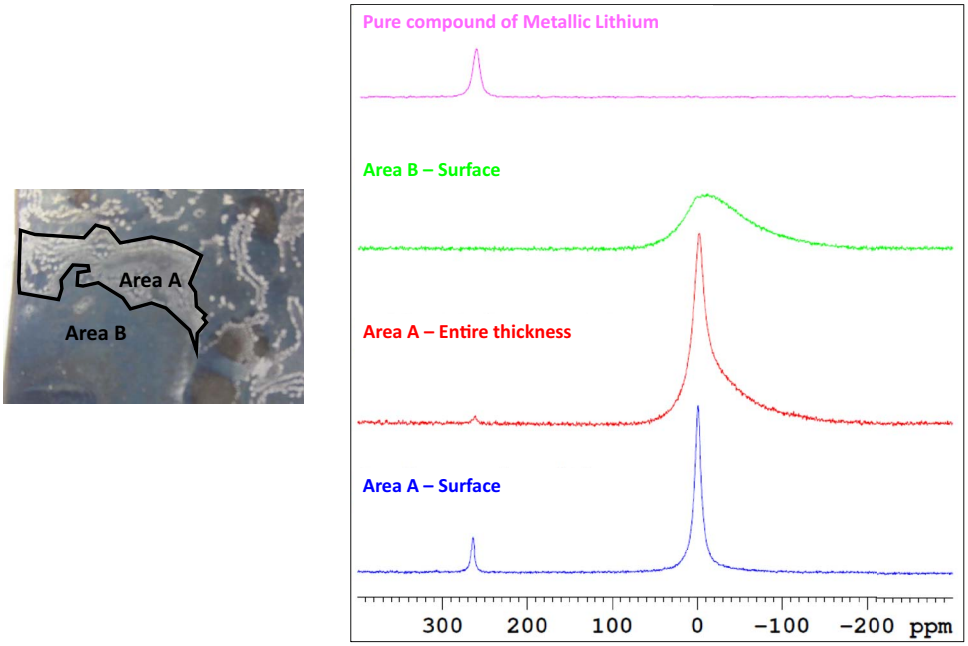

Figure 4. ^{7}Li NMR analysis: Metallic lithium detection on graphite electrode after calendar aging (4 months of storage: T=60°C and SOC=100%) including 6 periodic electric check-ups. Area A: area with lithiated deposits. Area B: area without lithiated deposits.

separator shows the same white symmetrical areas and the corresponding gray stains observed on both positive and negative electrodes. However, there are no presence of metallic lithium on graphite electrodes. Both cells aged with or without periodic check-up tests have been stored in the same condition (at 60°C and at 100% of SOC; during 4 months and until a SOH of 75% and 82% respectively). The difference of SOH between the two cells can most likely be attributed to the lithium loss caused by the intermediate check-up tests which are leading to the metallic lithium deposits.

According to the literature, at least two explanations can be proposed regarding the brown coloration found on the separator. It could be due to either remaining lithiated graphite and/or linked to the thermal and electrochemical degradation of $LiPF_6$.[45–46] Nagasubramanian observed discoloration of the electrolyte containing $LiPF_6$ and based on solvents such as ethylene carbonate (EC) and ethyl methyl carbonate (EMC) at 60°C while electrolyte containing $LiN(SO_2C_2F_5)_2$ showed very little discoloration even at 120°C.[45] Zhang et al. reported that 1.2 M $LiPF_6$ 3:3:4 PC/EC/EMC electrolyte had changed its color to brown after 2 weeks of storage at 60°C.[46] Similarly, a piece of a fresh separator has been immersed in an electrolyte composed by 1M $LiPF_6$ EC/EMC at 45°C for one month. In this experiment, we observed that the electrolyte became brown but the separator stayed white. So, it can be concluded that the thermal decomposition of $LiPF_6$ is not sufficient to modify the color of the separator. Brown color appears only when the separator is in contact with electrodes as confirmed by visual inspection. Namely, the upper surface of separator not in contact with electrodes is still white. To go further in the understanding of the emergence of the distinct brown coloration of the separator, a piece of polyethylene in contact with lithiated graphite electrode and another piece in contact with delithiated NMC electrode were stored in an electrolyte composed by 1M $LiPF_6$ EC/EMC during one month at 45°C. It was observed that only polyethylene in contact with delithiated NMC has changed its color to brown. It is reasonable to assume that white areas found in large amounts on brown separators retrieved from cells aged at 45°C and 60°C have thus not been in close contact with the NMC surface.

This contact disconnection is probably due to the progressive formation of gas bubbles caused by the degradation of the electrolyte inside the cell. Gas formation may be due to the electrolyte components oxidation at the NMC electrode maintained at high potential (calendar storage at SOC=100%) as reported in the literature.[47,48] Jalkanen et al. suggested that gas formation is the reason for local Li deposition after cycling at high temperature.[20]

Deposit analysis by lithium-7 nuclear magnetic resonance.— Figure 4 illustrates ^{7}Li NMR measurements performed on graphite electrode retrieved from the cell aged in calendar mode at 60°C and 100% of SOC. Samples were chosen as followed: 1) In the region of lithiated deposits (area A), only at the extreme surface of the electrode. 2) In the region of lithiated deposits (area A), in the thickness of the electrode. 3) At the electrode surface in any region without lithiated deposits (area B).

With a specific signal centered at 260 ppm, the ^{7}Li NMR spectra demonstrated the presence of metallic lithium only where lithiated deposits could be picked out. This signal is visible both when the material was collected by scraping the surface (area A) of the electrode or by taking the thickness (area A) of the electrode. In the latter case the intensity of the signal was lower because of dilution effects (see Figure 4). According to the literature, the observed signal corresponds to a clear signature of Li metal with this technique.[40] This observation is also in accordance with complementary GD-OES depth profiling measurements of the electrodes from the same cell aged at 45°C and SOC = 100%. These results will be published in a future paper. For the other spectrum, a signal at 0 ppm can be observed. This signal is narrow when it corresponds to a sample scraped at the surface of lithiated deposits (area A). However, if the sample is taken in the thickness (area A) of lithiated deposits, a broad shoulder appears at higher field in the range 0 to −100 ppm. Very interestingly, if the sample is taken at the surface (area B) outside lithiated deposits only the broad signal is observed. On one hand, taking into account the NMR data reported in literature for ^{7}Li, the signal at 0 ppm can easily be assigned to lithium in diamagnetic compound complexes with graphite derivatives for instance or diamagnetic inorganic salts. On the other hand, the broad signal ranging from 0 to 100 ppm could be assigned to paramagnetic inorganic compounds including Ni, Mn Cr or Co. The fact that the signal remains broad even at high spinning rate of the sample (50 kHz) and at moderated magnetic field (4.7 T) is consistent with a large number of different compounds with rather disordered structures leading to a complete loss in the resolution.

Table I. Content (%) of additive per time of storage in function of the sum of all detected carbonates.

Materials	With periodic check-ups			Without periodic check-up
	Fresh	cal@25°C	cal@45°C	cal@60°C
EMC + EC + other detected carbonates	100.00	100.00	100.00	100.00
VC	0.12	0.00	0.00	0.00
FEC	1.02	0.08	0.04	0.07
Biphenyl	12.28	1.34	0.64	2.55
1,3-PS	2.79	0.26	0.10	0.13

Content (%) of each component

Type	Component	With periodic check-ups			Without periodic check-up
		Fresh	cal@25°C	cal@45°C	cal@60°C
Solvents	EMC	53.52	49.20	46.45	53.52
	EC	32.53	32.53	32.53	21.66
Additives	VC	0.10	0.00	0.00	0.00
	FEC	0.88	0.62	0.34	0.21
	Biphenyl	10.57	9.98	5.23	7.84
	1,3-PS	2.40	1.95	0.84	0.40
Decomposition products	DMC	0.00	0.00	0.28	0.29
	DEC	0.00	0.00	1.14	0.88
	2-methoxycarbonyloxyethyl methyl carbonate	0.00	0.00	0.06	0.00
	2-ethoxycarbonyloxyethyl methyl carbonate	0.00	0.00	0.00	0.46
Gas and/or non detected material		0.00	5.73	13.13	14.74

Note that this broad signal is dominant for a spectrum of material scrapped at the electrode surface, they could be formed by reaction with degradation products for the positive electrode.

There is a low intensity peak corresponding to metallic lithium (260 ppm) when the entire thickness area A is considered. Here, the peak corresponding to lithium in oxidized form (at 0 ppm) is the sum between the one observed with area A (scrapping surface) and the one observed with area B (entire thickness).

Effect of biphenyl additive in the electrolyte.—*Electrolyte analysis by Gas Chromatography – mass spectrometry.*—Additionally to analysis of electrode materials, the evolution of electrolyte components during aging was followed by GC-MS. A quantitative analyses of the electrolyte composition recovered from a fresh cell and from cells respectively aged in calendar mode (SOC=100%) at 25°C and 45°C with intermediate electric check-up tests during storage and at 60°C without any periodic capacity test is presented in Table I. Unfortunately, no GCMS has been performed for the ageing condition related to cell aged at T=60°C and SOC=100% with periodical check-ups. However, we can conclude from GCMS performed from samples recovered from cells aged at 25°C, 45°C, and 60°C (without intermediary check-ups). Original electrolyte components of the commercial pouch cell can be identified from the fresh electrolyte analysis as following: solvents (Ethyl Methyl Carbonate (EMC) and Ethylene Carbonate (EC)) and many additives (Vinylene carbonate (VC), Flueroethylene Carbonate (FEC), Biphenyl (BP) and 1,3-Propane Sultone (PS)).

The content of each additive in %, per time of storage, was calculated based on the sum of all detected carbonates. Other components are identified as originating from electrolyte decomposition for cells aged at 45°C and at 60°C: DMC, Diethyl Carbonate (DEC), ethyleneglycol bis-(methyl carbonate) or 2-methoxycarbonyloxyethyl methyl carbonate and 2-ethoxycarbonyloxyethyl methyl carbonate. DMC and DEC are generated by the reduction of EMC solvent on lithiated graphite surface.[49,50] The presence of ethyleneglycol bis-(methyl carbonate) (EGMC) is caused by the reaction between lithium alkoxides and EC.[51] VC additive is totally consumed with aging, FEC and 1,3-PS show lower concentrations.

Biphenyl concentration has decreased significantly at 45°C and at 60°C. The decrease seems to be more at 45°C than at 60°C. This could be due to a shorter aging time and no periodic check up in the case of the cell aged at 60°C. Lithium plating is known to react with the electrolyte. The decrease of other additives can also be correlated to temperature.

There is a group of aromatic compounds such as biphenyl that show no reversible electrochemical behavior but give overcharge protection effects.[47] According to J. Garche et al., typical examples of this shutdown type are biphenyl or cyclohexylbenzene that polymerize on the cathode during overcharge and the liberated protons (H^+) migrate to the anode, generating hydrogen gas (H_2).[47] Biphenyl is suitable for use as an overcharge protective additive.[25,47,48,51–54] Zhang et al. reported that electro-polymerization of biphenyl at the temperature of 20 ± 5°C occurs at the overcharge potential of 4.5–5.5V to form a conductive organic layer on cathode surface.[51] Mao et al. reported the potential of polymerization of biphenyl at 4.7 V and at 21°C. Biphenyl polymerization generates gas increasing the internal cell pressure. This phenomenon enables to disconnect the cell in case of overcharge.[48] For example, the excessive gas pressure would open the safety cap for certain cell designs.[31,54,55] However, up to our knowledge, the literature does not mention polymerization of biphenyl at high temperature in a Graphite/NMC lithium-ion system.

The decreasing in the biphenyl concentration results from its polymerization process. This leads to drying-out areas of the separator visible in form of white stains which will be symmetrically impregnated on the surface of both electrodes (Figure 2).

Post-mortem analysis of coin cells: electrolyte with and without biphenyl as an additive.—To go further in this study, the effect of the biphenyl additive in the electrolyte is investigated with CR2032 coin cells based on pristine NMC and graphite electrodes and Celgard 2400 separator. Figure 5 shows the visual inspection of coin cell components after the storage at 45°C and at SOC=100% during 25 days with a periodic check-up test every 4 days. Similar white zones are observed in the case of coin cells containing biphenyl as an additive in the electrolyte. Depositions of lithium metal are found on the graphite electrodes originating from this cell. These circular depositions are similar to those observed with the commercial 16 Ah pouch cells (see Figure 2). It should be noted that the components recovered from the coin cell without the biphenyl additive show no evidence of degradation. Therefore, this result confirms that the reaction of the biphenyl additive is the origin of the lithium deposition observed on the graphite electrodes of the commercial 16 Ah C/NMC Li-ion cells in calendar aging at 45°C and 60°C at SOC=100%.

Electrolyte composition	Components			Comments
	Pristine Graphite	Celgard® 2400 Separator	Pristine NMC	
1:1:1: wt EC:DMC:EMC + 1M $LiPF_6$				No Lithium deposition
1:1:1: wt EC:DMC:EMC + 1M $LiPF_6$ + 2%wt of Biphenyl				Lithium deposition

Figure 5. Visual inspection of Graphite/NMC coin cells components after calendar aging (25 days of storage: T=45°C and SOC = 100%) including periodic electric check-up tests every 4 days. Metallic lithium deposits are found on graphite electrodes recovered from coin cell that contains biphenyl.

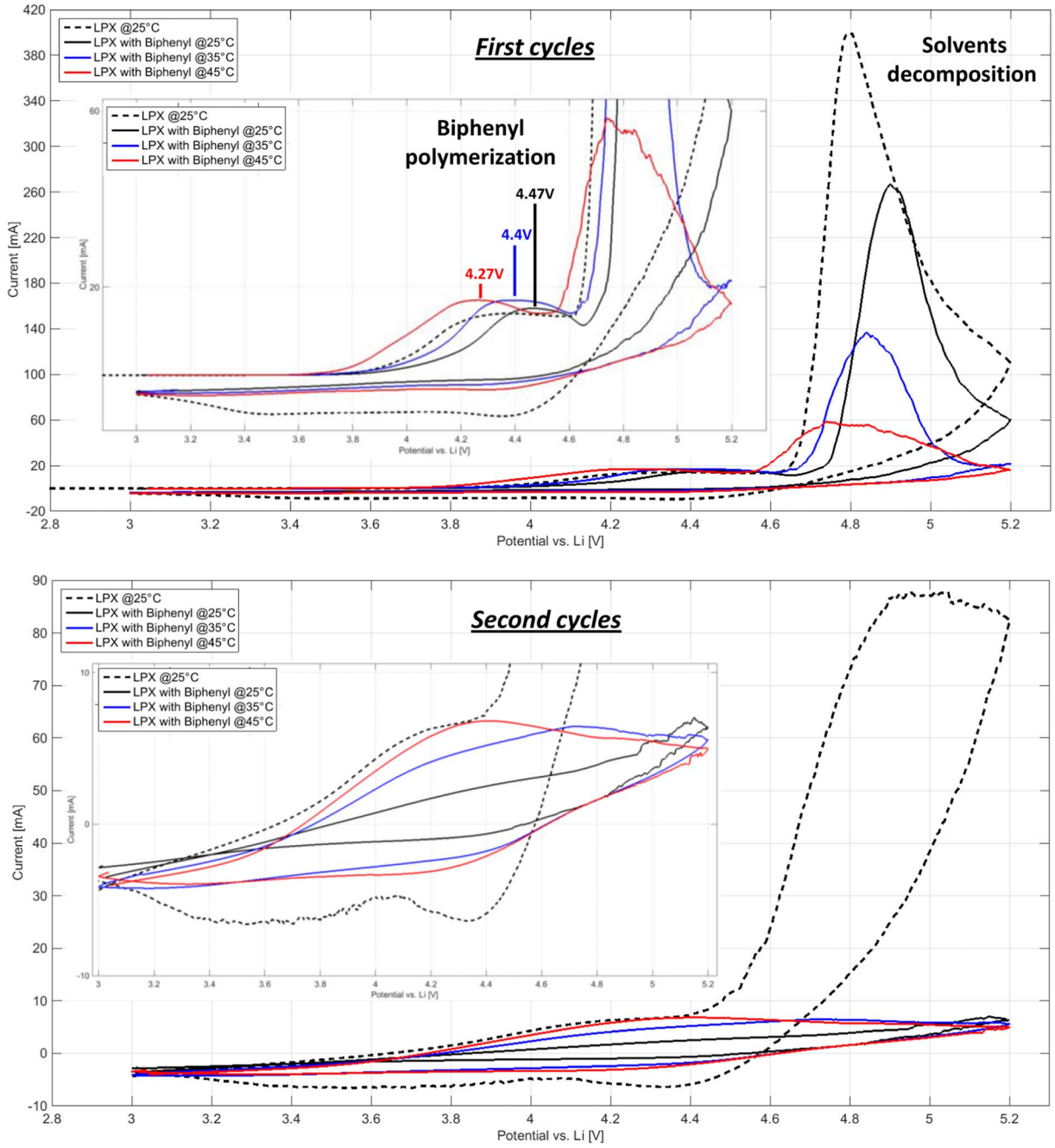

Figure 6. Effects of the temperature increasing on biphenyl polymerization potentials. The second cycles show that the electrolyte is hindered by the polymer on the NMC surface in the case of coin cells that contain biphenyl.

Post-mortem analysis of coin cells: cyclic voltammetry.—As indicated above, the effect of increasing temperature on biphenyl polymerization is not well understood. Cyclic voltammetry measurements of four additional CR2032 coin cells based on pristine NMC electrode, metal lithium electrode, and Celgard 2400 separator have been performed in order to measure the polymerization potential of this aromatic component at elevated temperatures. Figure 6 highlights that the polymerization of biphenyl occurs around 4.47 V vs Li/Li^+ at 25°C, 4.4 V vs. Li/Li^+ at 35°C and 4.27 V vs Li/Li^+ at 45°C.

The second peak at higher potential (with higher intensity) corresponds to the decomposition of electrolyte solvents. Nevertheless, the polymerization starts at 3.8 V at 45°C to reach a peak at around 4.3 V. In the case of commercial cells stored at 45°C and 60°C and at SOC = 100%, biphenyl has certainly polymerized at potentials much lower than 4.5 V vs. Li/Li^+ (overcharge potential at 21°C as suggested by Mao et al.[48]) leading to the observed local lithium deposition on graphite electrodes of the 16 Ah pouch cells.

We note that the cell voltage is equal to 4.2 V when it is stored at 100% of SOC. This means that the potential of NMC can reach 4.3 V vs. Li/Li^+, triggering the polymerization of biphenyl at high temperature. During the second cycle, the peak corresponding to solvent decomposition is very weak and flattened for biphenyl containing coin cells. The electrolyte oxidation must be hindered by the polymer on the NMC surface.[56]

The two coin cells measured at 25°C were disassembled for visual inspection as illustrated in Figure 7. The NMC electrode and separator of the coin cell without biphenyl does not show significant defects.

Electrolyte composition	Components	
	Pristine NMC	Celgard® 2400 Separator
1:1:1: wt EC:DMC:EMC + 1M $LiPF_6$		
1:1:1: wt EC:DMC:EMC + 1M $LiPF_6$ + 2%wt of Biphenyl		

Figure 7. Visual inspection of Li metal/NMC coin cells components after two cycles of cyclic voltammetry at 25°C. The separator of the coin cell containing biphenyl presents the same morphology than commercial cells separators aged at 45°C and 60°C in calendar mode.

The coin cell containing biphenyl presents white areas on the NMC electrode surface and its separator turned brown. It is noteworthy that the brown coloration of the separator appears stronger in presence of biphenyl. A complementary study is ongoing and will be the subject

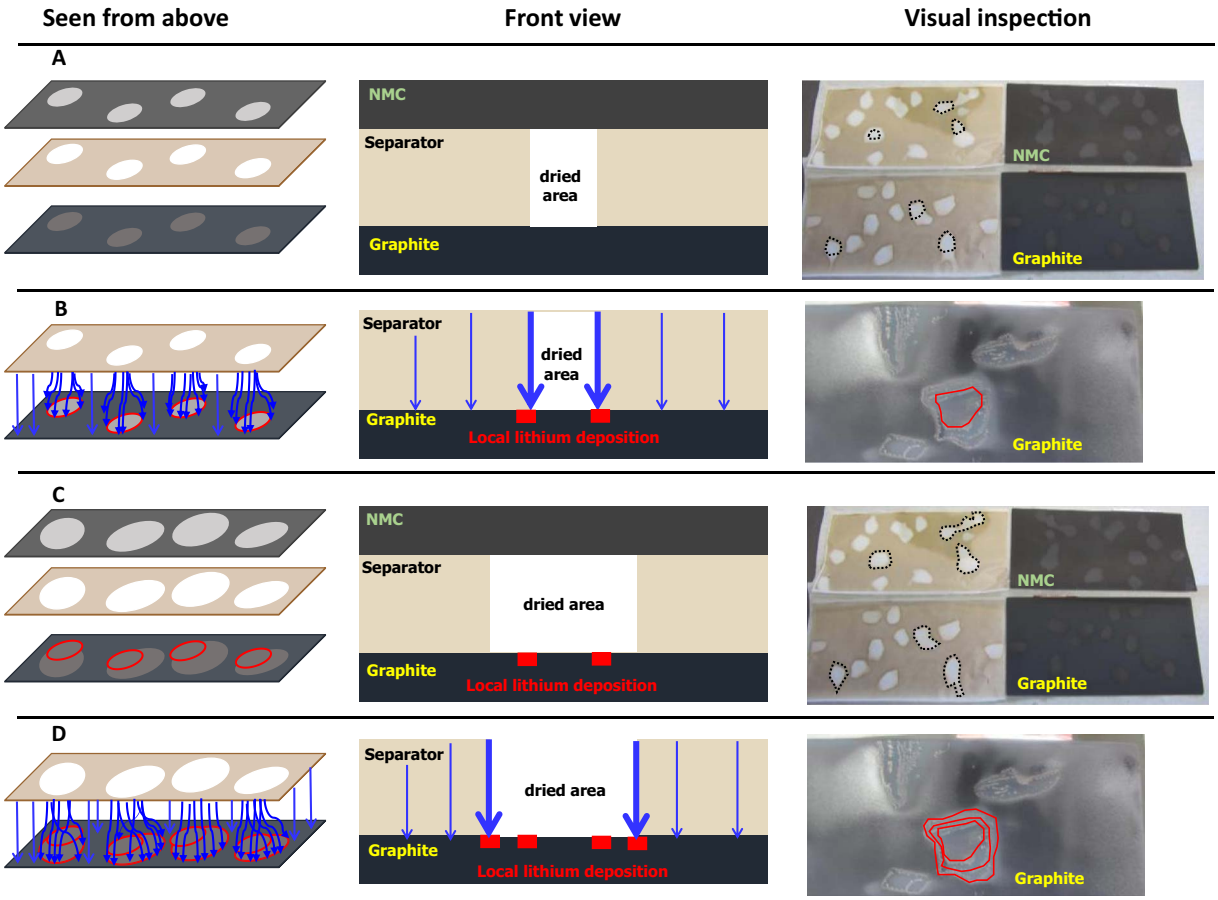

Figure 8. Lithium plating development process in high temperature conditions with biphenyl-containing electrolyte in Graphite/NMC Li-ion cell. Step A: The polymerization of Biphenyl during the storage at high temperature and at high state of charge leads to the production of gas bubbles and the decreasing of its concentration in the electrolyte. White dried zones found on the separator, which has turned brown, symmetrically impregnate both electrodes surfaces. Step B: It is in the border of these impregnated areas on graphite electrode that lithium metal is deposited during check-up tests due to the high local current density. Step C: During the following storage periods, if the electrolyte degradation continues, these dried areas could expand and / or move inside the cell. Step D: Thus, during each capacity test, new lithium depositions are formed. This explains the presence of several concentric metallic lithium depositions nearby.

in a forthcoming publication. The same morphology was found on commercial cells after calendar aging at high temperature (see Figure 2 and Figure 3). We suggest that at high temperature, biphenyl could polymerize at lower voltages (without overcharge), leading to gas formation, which generates local electrolyte depletion in the separator that creates white zones.

Model of Local Li Metal Deposition at High Temperature

Figure 8 presents a scheme that explains the formation of local lithium metal deposition in calendar aging at high temperature and high state of charge. During the storage period at elevated temperature (above ∼45°C) and at high state of charge (at around 100% of SOC), the potential of the positive electrode vs. Li/Li^+ is at its highest level. At this temperature, biphenyl additive can polymerize and generate gas inside the cell. The progressive formation of gas bubbles causes a contact disconnection between the electrodes and the separator, especially in the areas where those bubbles are formed. This creates insulated zones separating the two electrodes. Due the "stacked" geometry of cells, these white dried zones on the separator symmetrically impregnate both electrodes surfaces (Step A). These dried zones are very resistive and then the current will be forced to pass through the border of these latter regions. During the periodic check-up test performed at 25°C, metallic lithium is then deposited on the border of these dried zones due to the local high current density and the resulting local negative potential vs. Li/Li^+ (Step B). If the storage period at high temperature and high state of charge is prolonged then biphenyl polymerization may evolve over time, forming larger dried zones (Step C) that will create additional metallic lithium depositions at each check-up test (Step D). This explains the presence of several concentric lithium depositions nearby. This explains also the lower capacity of the cell with check-ups at 60°C compared to the cell without check-ups. In the calendar aging test without check-ups, although the same white dried areas were observed on the separator and on the surface of the NMC electrode, absolutely no lithium deposition was found on graphite electrode.

Conclusions

Unexpected localized metallic lithium depositions were found on top of graphite electrodes of commercial 16 Ah Li-ion pouch cells after calendar aging at high temperature and high state of charge. We determined that the presence of the biphenyl additive contained in the electrolyte in combination with periodic capacity tests are at the origin of this degradation mechanism. Polymerization of biphenyl results in the formation of a gas that can occur at 45°C when the voltage of the positive electrode reaches 4.27 V vs Li/Li^+, corresponding to the calendar aging conditions used in our work (45 and 60°C; 100% SOC). The polymerization reaction is irreversible and results in electrolyte-free zones which are highly resistive to ion transport. During periodic capacity tests, high current densities are generated at the circumference of these zones leading to Lithium metal depositions. Even though the lithium depositions do not lead to cell failure, it strongly reduces the discharge capacity by lithium trapping and inactivation. This aging protocol can be compared to the use of Li-ion cells in applications such as electric vehicles with long rest time (calendar aging) and regular cycling phases (periodic capacity tests). It is therefore imperative for the EV industry to perform similar protocols to test the battery in 'real life' operation.

Acknowledgments

The research leading to these results was performed within the MAT4BAT project (http://mat4bat.eu/) and received funding from the European Community's Seventh Framework Program (FP7/2007-2013) under grant agreement n°608931. We thank Dr. J. Kaiser (KIT), Dr. César Gutiérrez Couceiro (CIDETEC), Dr. Khiem Trad (VITO)and Dr. Sébastien Grolleau (EIGSI) for helpful discussions. This project has received support from the State Program "Investment for the Future" bearing the reference (ANR-10-ITE-0003). Post-mortem analyses of the 16Ah cells were conducted at CIC, ZSW and CEA. GC-MS, NMR measurements and tests with coin cells were performed by CEA.

References

1. J. Jaguemont, L. Boulon, and Y. Dubé, A comprehensive review of lithium-ion batteries used in hybrid and electric vehicles at cold temperatures, *Applied Energy.*, **164**, 99 (2016).
2. B. Diouf and R. Pode, Potential of lithium-ion batteries in renewable energy, *Renewable Energy.*, **76**, 375e380 (2015).
3. G. Caillon, Accumulateurs portables, *Techniques de l'Ingénieur.*, **E2140** (2001).
4. M. Petzl and M. A. Danzer, Nondestructive detection, characterization, and qualification of lithium plating in commercial lithium ion batteries, *J. Power Sources.*, **254**, 80 (2014).
5. M. Petzl, M. Kasper, and M.A. Danzer, Lithium plating in a commercial lithium-ion battery – A low-temperature aging study, *J. Power Sources.*, **275**, 799 (2015).
6. S. Schindler, M. Bauer, M. Petzl, and M.A. Danzer, Voltage relaxation and impedance spectroscopy as in-operando methods for the detection of lithium plating on graphitic anodes in commercial lithium-ion cells, *J. Power Sources.*, **304**, 170 (2016).
7. M. C. Smart and B. V. Ratnakumar, Effects of electrolyte composition on lithium plating in lithium-ion cells, *J. Electrochem. Soc.*, **158**(4), A379 (2011).
8. P. Maire, A. Evans, H. Kaiser, W. Scheifele, and P. Novák, Colorimetric determination of lithium content in electrodes of lithium-ion batteries, *J. Electrochem. Soc.*, **155**(11), A862 (2008).
9. M. Wakihara and O. Yamamoto, *Lithium ion batteries: Fundamentals and Performance*, Kodansha (1998).
10. H. Zheng, L. Tan, L. Zhang, Q. Qu, Z. Wan, Y. Wang, M. Shen, and H. Zheng, Correlation between lithium deposition on graphite electrode and the capacity loss for LiFePO4/graphite cells, *Electrochimica Acta.*, **173**, 323 (2015).
11. *NASA Engineering and Safety Center Technical Report*, NASA Aerospace Flight Battery Program, RP-08-75.
12. L.-E. Downie, L.-J. Krause, J.-C. Burns, L.-D. Jensen, V.-L. Chevrier, and J.-R. Dahn, In situ detection of lithium plating on graphite electrodes by electrochemical calorimetry, *J. Electrochem. Soc.*, **160**(4), A588 (2013).
13. J.-C. Burns, D.A. Stevens, and J.-R. Dahn, In situ detection of lithium plating using high precision coulorimetry, *J. Electrochem. Soc.*, **162**(6), A959 (2015).
14. J. Cannarella and C. B. Arnold, The effects of defects on localized plating in Lithium-ion Batteries, *J. Electrochem. Soc.*, **162**(7), A1365 (2015).
15. V. Agubra and J. Fergus, Lithium Ion Battery Anode Aging Mechanisms, *Materials*, **6**, 1310 (2013).
16. Z. Li, J. Huang, B. Y. Liaw, V. Metzler, and J. Zhang, A review of lithium deposition in lithium-ion and lithium metal secondary batteries, *J. Power Sources.*, **254**, 184 (2014).
17. Z. Guo, J. Zhu, J. Feng, and S. Du, Direct in situ observation and explanation of lithium dendrite of commercial graphite electrodes, *RSC Adv.*, **5**, 69514 (2015).
18. T. Waldmann, B-I. Hogg, M. Kasper, S. Grolleau, C. Gutiérrez Couceiro, K. Trad, B. Pilipili Matadi, and M. Wohlfahrt-Mehrens, Interplay of Operational Parameters on Lithium Deposition in Lithium-ion cells: Systematic Measurements with Reconstructed 3-Electrode Pouch Full Cells, *J. Electrochem. Soc.*, **163**(7), A1 (2016).
19. T. Waldmann, M. Kasper, M. Wohlfahrt-Mehrens, and Optimization of Charging Strategy by Prevention of Lithium Deposition on Anodes in high-energy Lithium-ion Batteries - Electrochemical Experiments, *Electrochimica Acta.*, **178**, 525 (2015).
20. K. Jalkanen, J. Karppinen, L. Skogström, T. Laurila, M. Nisula, and K. Vuorilehto, Cycle aging of commercial NMC/graphite pouch cells at different temperatures, *Applied Energy.*, **154**, 160 (2015).
21. M. Gauthier, T.J. Carney, A. Grimaud, L. Giordano, N. Pour, H-H. Chang, D. P. Fenning, S.F. Lux, O. Paschos, C. Bauer, F. Maglia, S. Lupart, P. Lamp, and Y. Shao-Horn, Electrode-Electrolyte Interface in Li-ion Batteries: Current Understanding and New Insights, *J. Phys. Chem. Lett.*, **6**, 4653 (2015).
22. D. Takamatsu, Y. Orikasa, S. Mori, T. Nakatsutsumi, K. Yamamoto, Y. Koyama, T. Minato, T. Hirano, H. Tanida, H. Arai, Y. Uchimoto, and Z. Ogumi, Effect of an electrolyte additive of vinylene carbonate on the electronic structure at the surface of a lithium cobalt oxide electrode under battery operating conditions, *J. Phys. Chem. C*, **119**, 9791 (2015).
23. E. Markevich, G. Salitra, K. Fridman, R. Sharabi, G. Gershinky, A. Garsuch, G. Semrau, M.A. Schimdt, and D. Aurbach, Fluoroethylene carbonate as important component in electrolyte solutions for high-voltage lithium batteries: role of surface chemistry on the cathode, *Langmuir*, **30**(25), 7414 (2014).
24. D. Aurbach, Y. Talyosef, B. Markovsky, E. Markevich, E. Zinigrad, L. Asraf, J.S. Gnanaraj, and H.-J. Kim, *Design of electrolyte solutions for Li and Li-ion batteries: a review*, Electrochemical Acta (2004).
25. S. S. Zhang, A review of electrolyte additives for lithium-ion batteries, *J. Power Sources.*, **162**, 1379 (2006).
26. Y. Ein-Eli, Dimethyl carbonates (DMC) electrolytes - the effect of solvent purity on Li-ion intercalation into graphite anodes, *Electrochemistry communications*, **4**, 644 (2002).
27. B. Zhang, M. Metzger, S. Solchenbach, M. Payne, S. Meini, H.A. Gasteiger, A. Garsuch, and B.L. Lucht, Role of 1,3-propane sultone and vinylene carbonate in solid electrolyte interface formation and gas generation, *J. Phys. Chem, C*, **119**, 11337 (2015).
28. T. R. Jow, K. Xu, O. Borodin, and M. Ue, Electrolytes for lithium and lithium-ion batteries, *Johnson Matthey Technol. Rev.*, **59**(1), 30 (2015).

29. W. A. van Schalkwijk and B. Scrosati, *Advances in lithium-ion batteries*, Klumer Academics Publishers, 155.
30. R. Imnhof and P. Novák, Oxydative electrolyte solvent degradation in lithium-ion batteries: an in situ differencial electrochemical mass spectrosmetry investigation, *J. Electrochem. Soc.*, **146**(5), 1702 (1999).
31. M. Fleischhammer, T. Waldmann, G. Bisle, B-I. Hogg, and M. Wohlfahrt-Mehrens, Interaction of cyclic aging at high-rate and low temperatures and safety in lithium-ion batteries, *J. Power Sources.*, **274**, 432 (2015).
32. W-J. Zhang, A review of the electrochemical performance of alloy anodes for lithium-ion batteries, *J. Power Sources.*, **96**, 13 (2011).
33. J. Zhou and P. H. L. Notten, Development of reliable lithium microreference electrodes for long-term in situ studies of lithium-based battery systems, *J. Electrochem. Soc.*, **151**(12) A2173 (2004).
34. M. Hahn, H. Buqa, P.W. Rush, D. Goers, M. E. Spahr, J. Ufheil, P. Novák, and R. Kötz, A dilatometric study of lithium intercalation into powder-type graphite electrodes, *Electrochem. Solid-State Lett.*, **11**(9), A151 (2008).
35. J.I. Yamaki, M. Egashira, and S. Okada, Potential and thermodynamics of graphite anodes in Li-ion cells, *J. Electrochem. Soc.*, **147**(12), A460 (2000).
36. N. Ghanbari, T. Waldmann, M. Kasper, P. Axmann, and M. Wohlfahrt-Mehrens, Detection of Li Deposition by Glow Discharge Optical Emission Spectroscopy in Post-Mortem Analysis, *Electrochemical and Solid-State Letters*, **4**(9), A100 (2015).
37. M. Ecker, N. Nieto, S. Käbitz, J. Schmalstieg, H. Blanke, A. Warnecke, and D. Uwe Sauer, Calendar and cycle life study of Li(NiMnCo)O2-based 18650 lithium-ion batteries, *J. Power Sources.*, **248**, 839 (2014).
38. P. Keil, S. F. Schuster, J. Wilhem, J. Travi, A. Hauser, R. C. Karl, and A. Jossen, Calendar Aging of Lithium-Ion Batteries I. Impact of the Graphite Anode on Capacity Fade, *J. Electrochem. Soc.*, **163**(9), A1872 (2016).
39. J. Arai, Y. Okada, T. Sugiyama, M. Izuka, K. Gotoh, and K. Takeda, In Situ Solid State 7Li NMR Observations of Lithium Metal Deposition during Overcharge in Lithium Ion Batteries, *J. Electrochem. Soc.*, **162**(6), A952 (2015).
40. R. Bhattacharyya, B. Key, H. Chen, A. S. Best, A. F. Hollenkamp, and C. P. Grey, In situ NMR observation of the formation metallic lithium microstructures in lithium batteries, *Nature Materials.*, **9**, 504 (2010).
41. K. Amine, J. Liu, and I. Belharouak, High-temperature storage and cycling of C-LiFePO4/graphite Li-ion cells, *Electrochemistry communications*, **7**, 669 (2005).
42. S. Grolleau, A. Delaille, H. Gaulous, P. Gyan, R. Revel, J. Bernard, E. Redondo-Iglesias, and J. Peter, On behalf of the SIMACL Network, Calendar aging of commercial graphite/LFP cell - Predicting capacity fade under time dependent storage conditions, *J. Power Sources.*, **225**, 450 (2014).
43. S. Käbitz, J. B. Gerschler, M. Ecker, Y. Yurdagel, B. Emmermacher, D. André, T. Mitsch, and D. Uwe Sauer, Cycle and calendar life study of a graphite|LiNi1/3Mn1/3Co1/3O2 Li-ion high energy system. Part A: Full cell characterization, *J. Power Sources.*, **239**, 572 (2013).
44. M. Ecker, J. B. Gerschler, J. Vogel, S. Käbitz, F. Hust, P. Dechent, and D. Uwe Sauer, Development of a lifetime prediction model for lithium-ion batteries based on extended accelerated aging test data, *J. Power Sources.*, **215**, 248 (2012).
45. N. Nagasubramanian, Comparison of the thermal and electrochemical properties of LiPF6 and Li(SO2C2F5)2 salts in organic electrolytes, *J. Power Sources.*, **119–121**, 811 (2003).
46. S. S. Zhang, K. Xu, and T. R. Jow, A thermal stabilizer for LiPF6-based electrolytes of Li-ion cells, *Electrochemical and Solid-State Letters*, **5**(9), A206 (2002).
47. J. Garche, C. K. Dyer, P. T. Moseley, Z. Ogumi, D.A. J. Rand, and B. Scrosati, *Encyclopedia of Electrochemical Power Sources, Secondary Batteries – Lithium Rechargeable Systems / Electrolytes: Nonaqueous*, Elsevier p. 80-81, Science (2009).
48. H. Mao and U. Sacken, U.S. Pat. 5,776,627 (1998).
49. G. Gachot, S. Grugeon, M. Armand, S. Pilard, P. Guenot, J-M. Tarascon, and S. Laruelle, Desciphering the multi-step degradation mechanisms of carbonate-based electrolyte in Li batteries, *J. Power Sources.*, **178**, 409 (2008).
50. H. Kim, S. Grugeon, G. Gachot, M. Armand, L. Sannier, and S. Laruelle, Ethylene bis-carbonates as telltales of SEI and electrolyte health, role of carbonate type and new additives, *Electrochimica Acta.*, **136**, 157 (2014).
51. Y. Zhang, A-Q. Zhang, Y-H. Gui, L-Z. Whang, X-B. Wu, C-F. Zhang, and P. Zhang, Application of biphenyl additive in electrolyte for liquid state Al-plastic film lithium batteries, *J. Power Sources.*, **185**, 492 (2008).
52. W. K. Behl, *Overcharge protection in ambient temperature lithium and lithium-ion cells - A literature survey*, Army Research Laboratory (1998) ARL-TR-1803.
53. C-H. Doh and A. Veluchamy, *Lithium ion batteries*, Chong Rae Park, Chap., **2** p 41 (2010).
54. K. Abe, T. Takaya, H. Yoshitake, Y. Ushigoe, M. Yoshio, and H. Wang, Functional electrolyte: additive for improving the cyclability of cathode materials, *Electrochem Solid-State Lett.*, **12**, A462 (2004).
55. N. Choi, J-G. Han, S.-Y. Ha, I. Park, and C.-K. Back, Recent advances in the electrolytes for interfacial stability of high-voltage cathodes in lithium-ion batteries, *RSC Adv.* **5**, 2732 (2015).
56. L. Xiao, X. Ai∗, Y. Cao, and H. Yang, Electrochemical behavior of biphenyl as polymerizable additive for overcharge protection of lithium ion batteries, *Electrochimica Acta.*, **49**, 4189 (2014).